 CMC, vol.11, no.2, pp.109-125, 2009

An Investigation into the Mechanical Behavior of Single-Walled Carbon Nanotubes under Uniaxial Tension Using Molecular Statics and Molecular Dynamics Simulations

Yeau-Ren Jeng[1], Ping-Chi Tsai[1], Guo-Zhe Huang[1] and I-Ling Chang[1]

Abstract: This study performs a series of Molecular Dynamics (MD) and Molecular Statics (MS) simulations to investigate the mechanical properties of single-walled carbon nanotubes (SWCNTs) under a uniaxial tensile strain. The simulations focus specifically on the effects of the nanotube helicity, the nanotube diameter and the percentage of vacancy defects on the bond length, bond angle and tensile strength of zigzag and armchair SWCNTs. In this study, a good agreement is observed between the MD and MS simulation results for the stress-strain response of the SWCNTs in both the elastic and the plastic deformation regimes. The MS simulations reveal that in the plastic deformation regime, the tensile strength of the armchair and zigzag SWCNTs increases with an increasing wrapping angle. In addition, it is shown that the tensile strength reduces significantly at larger values of the nanotube diameter. Moreover, it is observed that the tensile strength of both SWCNTs reduces as the percentage of defects within the nanotube structure increases. Finally, it is found that the results obtained from the molecular statics method are relatively insensitive to instabilities in the atomic structure, particularly in the absence of thermal fluctuations, and are in good agreement with the predictions obtained from the molecular dynamics method.

Keywords: Molecular statics, molecular dynamics, carbon nanotubes, mechanical properties, wrapping angle, vacancy percentage.

1 Introduction

Since their original discovery by Iijima in 1991 [Iijima (1991)], carbon nanotubes (CNTs) have attracted intensive interest throughout industry and academia. Experimental studies has shown that CNTs exist in a variety of structural configurations, including single-walled carbon nanotubes (SWCNTs) [Iijima and Ichlhashi

[1] Department of Mechanical Engineering, National Chung Cheng University, Chia-Yi 621, Taiwan

(1993); Bethune *et al*. (1993)], multi-walled carbon nanotubes (MWCNTs) [Ebbesen and Ajayan (1992); Zhao *et al.* (1997)], bundles [Qiu *et al.* (2003); Cheng *et al.* (1998)] and nanoropes [Thess *et al.* (1996); Cheng *et al.* (1998)]. Irrespective of their configuration, however, all CNTs are characterized by a remarkable degree of structural perfection, a small size, a low density, a high stiffness and mechanical strength, and excellent electronic, optical and transport properties [Yakobson *et al.* (1996); Jeng *et al.* (2007); Journet and Bernier (1998); Lau *et al.* (2004)]. As a result, CNTs have been extensively deployed in recent years for such diverse applications as memory chips, sensors, probes, tips, and reinforcement phase in composite materials.

However, the nanoscale dimensions of CNTs prevent the use of direct experimental techniques for measuring their mechanical properties, and thus theoretical computational simulations have emerged as the method of choice for characterizing their mechanical properties and obtaining detailed insights into the physical mechanisms governing their deformation. Of the various computational techniques available, one of the most commonly adopted is that of molecular dynamics (MD) simulations. Due to the availability of accurate inter-atomic potential data for a wide range of common engineering materials, MD simulations, in which the material of interest is modeled at the atomic level, provide a powerful technique for clarifying a wide range of complex physical phenomena in the microscale and nanoscale regimes. MD simulations assume that the instantaneous positions and velocities of the individual atoms within the system of interest conform to the principles of Newtonian mechanics, and thus the dynamic history of the assembly and the energy and force of the system are generated by numerically integrating the equations of motion of each atom at each time-step of the simulation procedure. Although MD simulations are commonly regarded as an ideal means of analyzing the mechanical response of engineering materials at the micro- or nanoscale, great care must be taken when specifying the simulation parameters in order to ensure the validity of the numerical results. For example, an improper treatment of the system temperature during the simulation process can greatly distort the numerical results, leading to solutions which are grossly higher or lower than those observed in practice [Zhang and Tanaka (1999); Cheong *et al.* (2001)]. Moreover, due to the complexity of the MD computations and the large time scales considered in most simulation systems, the application of MD simulations to large-scale systems comprising many hundreds or thousands of atoms is impractical if not completely unfeasible.

In MD simulations, it is assumed that the majority of the atoms move freely throughout the body of interest in accordance with Newton's law of motion. However, in condensed matter, the atoms and molecules actually oscillate thermodynamically

around their minimum energy positions, i.e. they have a quasi-static rather than dynamic characteristic. Accordingly, in recent years, a new class of simulation technique known as molecular statics (MS) has emerged [Jeng and Tan (2002)], in which the final relaxed configuration of the atomic structure is determined using an energy minimization technique. Studies have shown that the quasi-static characteristics of MS simulations yield a considerable improvement in the computational efficiency compared to that of MD simulations since the velocity components of the individual atoms within the system are ignored. As a result, the MS simulation approach has been increasingly employed in recent years as a means of gaining insights into the crystal lattice structure of common engineering materials under various conditions [Liu and Plimpton (1995); Jeng and Tan (2004a); Jeng and Tan (2004b); Jeng and Tan (2005); Jeng *et al.* (2006]. In practice, the choice of an appropriate molecular simulation approach (i.e. MD or MS) frequently comes down to a subjective decision on the part of the practitioner as to which technique can be expected to produce the most realistic results at an acceptable computational cost. Unfortunately, a review of the published literature reveals that no previous studies have utilized MS simulations to investigate the structural deformation of CNTs beyond their elastic limit during uniaxial deformation. Accordingly, this study performs a series of MS simulations using the Tersoff potential model [Tersoff (1986); Tersoff (1988)] to investigate the respective effects of the wrapping angle, the tube radius and the vacancy percentage on the tensile strength, bond length and bond angle of various zigzag and armchair SWCNTs. The applicability of the MS simulation approach is confirmed by comparing the simulations results obtained for the stress-strain response of the SWCNTs with those obtained using a conventional MD simulation technique.

2 Methodology

A SWCNT is a quasi one-dimensional system with the form of a graphite sheet rolled into a cylindrical shell [Iijima (1991); Iijima and Ichlhashi (1993); Bethune *et al.* (1993)]. Unlike the continuum shell model, a SWCNT comprises a series of hexagonal carbon rings, which collectively determine its physical and mechanical properties. A review of the related literature reveals that previous numerical investigations into the properties of SWCNTs have generally adopted the atomic calculation, Embedded Atom Method (EAM) or Tight-Binding (TB) formulation to model the various interactions which occur within the nanotube at the atomic scale [Shen and Atluri (2004a); Shen and Atluri (2004b); Ogata and Shibutani (2003); Brenner (1990)]. However, due to the large number of atoms within the SWCNT system and the long time scales considered in most simulation processes, the use of such quantum techniques to describe the atomic interactions is generally impractical due

to an excessive computational cost. Moreover, conventional finite element methods can not be applied at the atomic scale, and are therefore also unsuitable for modeling the properties of SWCNTs. Thus, as described above, MD simulations are widely regarded as the method of choice for analyzing the properties and deformation mechanisms of engineering materials at the micro- and nanoscale. However, since their time resolution is typically of the order of 1 ps or less, MD simulations are highly time-consuming when applied to the modeling of large-scale atomic systems. Consequently, the MS approach is commonly preferred when analyzing systems in which atomic fluctuations can be ignored. Since the velocity components of the individual atoms are neglected, MS simulations are more straightforward (and thus, more computationally efficient) than their MD counterparts, and therefore provide an ideal solution for modeling such complex phenomena as the size effect of thin films during nanoindentation [Jeng and Tan (2006)] and the structural deformation of nanowires [Chang and Chen (2007)]. Whereas MD simulations utilize Newtonian principles to compute the velocity and position of each atom at each time step in the simulation process, MS simulations use a conjugate gradient method to obtain the equilibrium atomic structure by minimizing the total energy within the system, i.e. the potential energy produced by inter-atomic interactions and the potential energy imparted to the system by external loading.

The current study performs a series of MS simulations to investigate the effects of the wrapping angle, the nanotube radius and the percentage of vacancy defects on the deformation behavior and mechanical strength of various zigzag and armchair SWCNTs under uniaxial tensile loading. For comparison and verification purposes, the stress-strain response of a zigzag SWCNT is also modeled using a MD simulation approach. In the simulations, the SWCNTs are initially relaxed by adjusting their periodic length in the x-direction so as to eliminate any residual stress. A uniform tensile strain is then applied in incremental steps of 0.5% in the axial direction, causing a uniform expansion of the periodic length in the direction of deformation. After each step of the loading process, the new equilibrium positions of the atoms within the simulation system are determined by applying the conjugate gradient method to minimize the total system energy.

In simulating the deformation of the SWCNTs, the carbon-carbon (C-C) interactions are modeled using the Tersoff potential [Tersoff (1986); Tersoff (1988)]. According to this model, the inter-atomic potential energy between two neighboring atoms i and j is formulated as

$$V_{ij} = f_c(r_{ij})[Aa_{ij}\exp(-\lambda_1 r_{ij}) - Bb_{ij}\exp(-\lambda_2 r_{ij})] \tag{1}$$

$$f_c(r_{ij}) = \begin{cases} 1, & r \le X - Y \\ \frac{1}{2} - \frac{1}{2}\sin\left[\frac{\pi}{2}\left(\frac{r-X}{Y}\right)\right], & X - Y < r \le X + Y \\ 0, & r > X + Y \end{cases} \tag{2}$$

where b_{ij} is a many-body bond-order parameter describing the effect exerted on the bond-formation energy between atoms i and $j$of the k nearest-neighbor atoms, i.e.

$$b_{ij} = \chi(1 + \zeta_{ij}^{n_i})^{-\frac{1}{(2n)}}, \tag{3}$$

Where

$$\zeta_{ij} = \sum_{K \neq i,j} f_c(r_{ij})\beta_i \varphi(\theta_{ijk}) \exp[\lambda_3^3 (r_{ij} - r_{ik})^3], \tag{4}$$

$$\varphi(\theta) = 1 + \frac{c^2}{d^2} - \frac{c^2}{[d^2 + (h - \cos\theta)^2]}, \tag{5}$$

$$a_{ij} = (1 + \alpha\omega_{ij})^{-\frac{1}{(2n)}}, \tag{6}$$

$$\omega_{ij} = \sum_{K \neq i,j} f_c(r_{ij}) \exp[\lambda_3^3 (r_{ij} - r_{ik})^3]. \tag{7}$$

In the equations above, ζ denotes the effective coordination number and $\phi(\theta)$ is a function of the angle between r_{ij} and r_{ik} and is fitted in such a way as to stabilize the tetrahedral structure. Finally, α and λ_3 are set equal to zero [Tersoff (1986)]. The remaining parameter values used in the present simulations are summarized in Table 1. Very recently, the theoretical study has succeeded in creating X-shaped molecular connections by welding achieved by electron beam irradiation of crossing SWCNTs [Jang *et al.* (2004)]. Latgé et al. [Latgé *et al.* (2005)] has studied the mechanical and thermal stability of Y-shaped junctions by using numerical simulations. Yakobson et al. [Yakobson *et al.* (2002)] also reported coalescence of fullerene cages and nanotube by the theoretical methods. Jeng and Tsai [Jeng and Tsai (2007)] also have carried out experimental and numerical investigation into buckling instability of carbon nanotube probes under nanoindentation. These excellent works demonstrate the feasibility of using classical molecular dynamic simulation based on a shorter cut length in the particular potential (Tersoff and/or Tersoff-Brenner). Although the accuracy of the Tersoff potential function does not match that of quantum-mechanical methods, it is nevertheless adopted in the present simulations because it is simple, computationally inexpensive, and has been successfully used for the purpose of qualitative estimates in previous studies [Jang *et al.* (2004); Latgé *et al.* (2005); Yakobson *et al.* (2002); Jeng and Tsai (2007)]. However, an important unresolved issue remains, namely the extent to which the results would be affected by the application of more robust potentials.

Table 1: Parameters used in Tersoff potential model

A (eV)	1393.6
B (eV)	346.74
λ_1 (Å^{-1})	3.4879
λ_2 (Å^{-1})	2.2119
β	1.5724×10^{-7}
n	0.72751
c	3.8049×10^{4}
d	4.3484
h	-0.57078
χ	1
X (Å)	1.95
Y (Å)	0.15

3 Results and discussion

3.1 Mechanical properties of single-walled carbon nanotubes under uniaxial tension

Figure 1(a) illustrates the variation of the tensile stress with the tensile strain in a zigzag (10,0) SWCNT as computed by the MS and MD simulation methods, respectively. It can be seen that the tensile stress of the SWCNT is clearly a function of the applied strain. Note that in both simulation methods, the axial tensile stress in the SWCNT was calculated by the cross-sectional ring area of the nanotube given an assumed equivalent wall thickness of 3.4 Å [Ebbessen and Ajayan (1992); Yu

et al. (2000a); Yu *et al.* (2000b)]. It can be seen that each of the three stress–strain curves has four distinct stages. In Stage 1, the tensile stress increases linearly with the tensile strain, i.e. the SWCNTs deform elastically. However, at a tensile strain of around 10%, the hexagonal cells all extend in the axial direction of the nanotubes, and that they do not return to their original geometries when the forces applied at either end of the structure are removed. This indicates that the nanotubes enter the plastic deformation regime (Stage 2). In Stage 3, the stress increases rapidly with increasing strain toward a peak value, corresponding to the maximum tensile strength (σ_{ts}) of the nanotube. When the strain is increased further, the C-C bonds in the nanotube fail, prompting the separation of the nanotube into two parts (Stage 4).

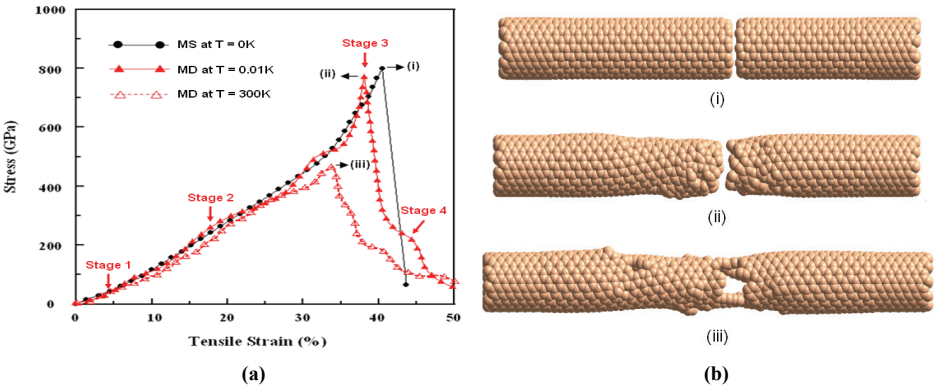

Figure 1: (a) Stress–strain curves of (10, 0) zigzag SWCNT as predicted by molecular statics and molecular dynamics simulations, respectively. (b) Typical snapshots of (10, 0) zigzag SWCNT under uniaxial strains corresponding to labels (i)–(iii) in Fig. 1(a). (Note that labels (i)–(iii) indicate positions of maximum stress used to determine maximum tensile strength of nanotube.)

From an inspection of the linear region of the stress-strain curves computed at a temperature of T = 0.01K, the Young's modulus (E_y) of the zigzag (10,0) SWCNT is determined to be 1.21 TPa when computed using the MS data, and 1.06 TPa when computed using the MD model. Moreover, it is observed that at a temperature of 0.01 K, a good agreement exists between the stress-strain profiles predicted by the two simulation methods in both the elastic and the plastic deformation regimes. From inspection, the difference in the values of σ_{ts} predicted by the two methods is found to be less than 5%. However, a notable difference is observed in the two sets of results at strains higher than that associated with the maximum mechanical strength. Specifically, the stress predicted by the MS method falls to a value

close to 0 GPa with virtually no further increase in the applied strain, whereas the stress predicted by the MD method reduces toward 0 GPa at a comparatively slower rate. It is thought that this discrepancy arises because the MS model computes the relaxed atomic structure of the nanotube solely on the basis of an energy minimization constraint, and therefore ignores the respective effects of bond rotation and competitive formations between the C-C bonds [Yakobson *et al.* (1998); Orlikowski (1999); Jeng *et al.* (2004)]. The Young's modulus computed using the MD model at a temperature of 300 K is found to have a value of 0.92 TPa, and is therefore lower than that computed using either the MS model or the MD model at a temperature of 0.01 K, i.e. 1.21 TPa and 1.06 TPa, respectively. This result is to be expected since materials generally have a higher stiffness at lower temperatures. Moreover, the result is consistent with that presented for SWCNTs under tension by Jeng *et al*. [Jeng *et al.* (2004)] and Shi *et al*. [Shi *et al*. (2002)]. Overall, it is observed that the MS stress-strain curve is smoother than the two MD curves. This can be attributed to the fact that the thermally-activated fluctuations in the atom positions in the SWCNT are taken into account in the MD simulations [Xie and Long (2006); Xie *et al.* (2007)], but are ignored in the MS model since an assumption is made that the atoms simply oscillate around their minimum-energy positions. A similar technique has also been successfully utilized to investigate into the nanoindentation size effects and mechanical contact behaviors of single asperities by *Jeng et al.* [Jeng and Tan (2006); Jeng *et al.* (2007)].

Figure 1(b) presents the atomic configurations of the (10,0) zigzag SWCNT under the tensile strains corresponding to labels (i)–(iii) in Fig. 1(a). In the upper snapshot, produced using the MS model, it is observed that the C-C bonds in the fracture region of the nanotube are extended in the axial direction and prevent the separation of the nanotube into two parts. However, when the strain is increased beyond that associated with the maximum mechanical strength of the nanotube, these C-C bonds fracture, and thus the stress within the tube reduces virtually instantaneously to zero (see Fig. 1(a)). The middle snapshot, produced using the MD model, is broadly similar to that produced by the MS model. However, a notably greater degree of atomic structural disorder is observed in the MD results due to the inclusion of C-C bond rotation and competitive formation effects in the simulation procedure. The lower snapshot, also produced using the MD model, shows that thermal effects and over-binding mechanisms have a significant effect upon the structural deformation behavior of the zigzag (10,0) SWCNT in the higher temperature regime. Specifically, it is observed that the higher temperature deformation conditions induce a necking effect in the nanotube and prompt the formation of a small number of one-atom chains in the fracture region of the tube. As the strain is increased, these chains are extended slightly in the axial direction before breaking

and thus, as shown in Fig. 1(a), the stress within the nanotube falls more slowly toward zero than that in the low-temperature tube in which no atomic chains are formed (see snapshot (ii) in Fig. 1(b)). Consequently, the present results indicate that the structural deformations of the SWCNTs are sensitive to temperature conditions. Note that these observations are consistent with the findings presented by Yakobson *et al*. [Yakobson *et al*. (1997)] and Chakrabart *et al*. [Chakrabart and Cagin (2008)].

The loading rate in MD simulations is much higher than that applied in practical experiments, and thus the effects of deformation-induced thermal fluctuations in the atomic configuration are overstated compared to those observed in the experimental case. However, the MS simulation model excludes the effects of the deformation-induced temperature rise and calculates the relaxed atomic configuration solely on the basis of the potential energy within the system. In other words, the MS method is insensitive to the effects of thermal instability and kinetic excitation [Zhang and Tanaka (1999); Cheong *et al.* (2001)], and can therefore be reasonably expected to provide an accurate representation of the low strain rate deformation of SWCNTs. Furthermore, as commented previously, an excellent agreement exists between the MS and MD stress–strain curves in both the elastic and the plastic deformation regimes (see Fig. 1(b)), and thus the MS approach provides a valid, computationally-efficient means of determining the basic mechanical properties of SWCNTs, e.g. the Young's modulus and Poisson's ratio.

Figure 2(a) illustrates the MS simulation results obtained for the variation of the stress with the tensile strain in the (10, 0) zigzag and (6, 6) armchair SWCNTs, respectively. To clarify the changes in the stress-strain response of the two nanotubes at different values of the applied strain, Fig. 2(b) presents snapshots of the unrolled graphitic networks of the two SWCNTs at strains corresponding to labels (I)–(III) and (i)–(iii) in Fig. 2(a), respectively. Figure 2(a) shows that for strains of less than approximately 10%, the two stress-strain curves overlap one another and are almost linear, i.e. both tubes are within the fully-elastic deformation regime. From inspection, the Young's modulus of the (10, 0) zigzag SWCNT is found to be 1.21 TPa, while that of the (6, 6) armchair SWCNT is determined to be 1.13 TPa. This result suggests that the lower bond angles in the zigzag tube (see snapshots (I) and (i) in Fig. 2(b)) are instrumental in increasing the nanotube stiffness. As the strain is increased beyond a value of 10%, a divergence is observed between the stress-strain profiles of the two nanotubes. Specifically, for a given value of the applied strain, the stress induced in the zigzag nanotube is higher than that induced in the armchair tube (see Fig. 2(a)). The snapshots presented in (II) and (ii) in Fig. 2(b) suggest that the difference in response of the two nanotubes is the result of geometric differences in the bond orientations of the two tubes. From an inspection

of Fig. 2(a), it is found that the zigzag CNT has a maximum stress of around 798 GPa at a strain of 41%, while the armchair CNT has a maximum stress of approximately 883 GPa at a strain of 46%. In other words, the armchair nanotube has a higher mechanical strength and undergoes a greater elongation prior to failure than the zigzag nanotube. Note that a similar phenomenon was reported for the yielding of SWCNTs under tension in the MD simulations performed by Zhang *et al.* [Zhang *et al.* (1998)]. As shown in Fig. 2(b), the principal bonds in the zigzag SWCNT are aligned with the tube axis, whereas those in the armchair SWCNT are inclined at an angle. As a result, the bonds in the zigzag nanotube experience a significant change in length under the effects of the applied uniaxial strain, whereas the bonds in the armchair nanotube tend to rotate initially under the effects of the applied load. Consequently, the bonds in the zigzag nanotube are more susceptible to breakage, and thus the tube fails at a lower strain than the armchair tube.

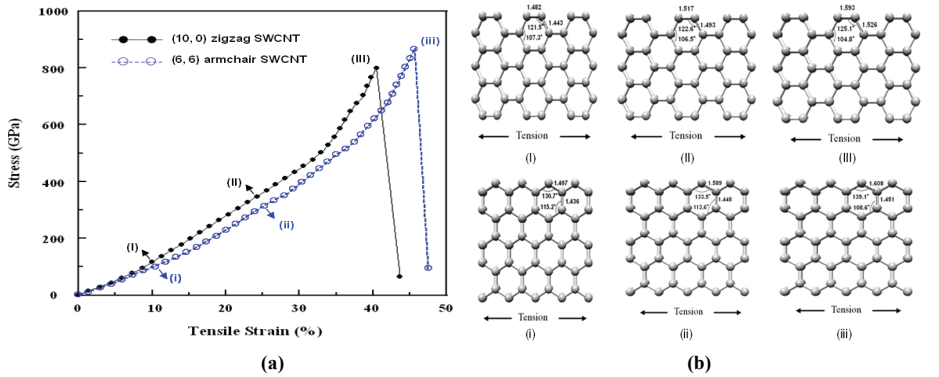

Figure 2: (a) Variation of stress with tensile strain for zigzag (10, 0) and armchair (6, 6) SWCNTs. (Note that labels (I)–(III) and (i)–(iii) denote different deformation stages of zigzag and armchair tubes, respectively, and correspond to snapshots presented in Fig. 2(b)). (b) Structural changes in zigzag (10, 0) and armchair (6, 6) SWCNTs during tensile testing. (Note that bond length measurements are given in angstroms while bond angles are given in degrees.)

3.2 Equations and mathematical expressionsInfluence of wrapping angle and size effect on mechanical properties of SWCNTs

Previous theoretical investigations have shown that the mechanical properties of a SWCNT, are insensitive to the helicity of the tube under small strains [Brenner *et al.* (1992); Yakobson *et al.* (1996); Lu (1997)]. However, at strains higher than

the yield strain, many materials deform plastically as a result of a significant distortion of the bonding topology [Ozaki *et al.* (2000); Jeng *et al.* (2004)], and thus it seems reasonable to speculate that the mechanical properties of a SWCNT may no longer be insensitive to the wrapping angle. To test this supposition, Fig. 3 plots the variation of the tensile strength of various (n, n) armchair and (n,m) zigzag SWCNTs. (Note that the simulation results are obtained using the MS model.) The results clearly show that for both types of nanotube, the maximum tensile strength increases with an increasing wrapping angle. Furthermore, it can be seen that the tensile strength is relatively insensitive to the size effect in nanotubes with a smaller diameter, but reduces significantly in the tubes with a diameter greater than 6.7 nm (e.g. the (n,m) zigzag CNT. This result is consistent with the findings of Tersoff and Ruoff [Tersoff and Ruoff (1994)] and is most likely attributed to the sagging characteristic of the tubular walls in SWCNTs. That is, the hollow structure of SWCNTs causes the tube to experience a certain degree of radial collapse, and therefore results in a loss in mechanical strength. The severity of the collapse increases with an increasing nanotube diameter, and thus the ultimate mechanical strength of SWCNTs reduces significantly when the diameter of the nanotube exceeds a certain critical value.

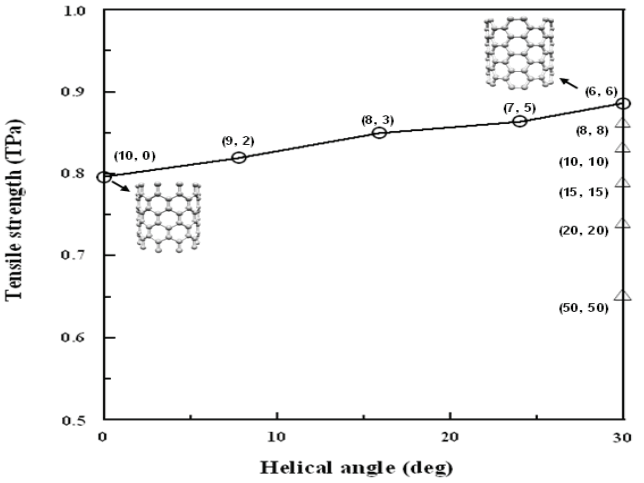

Figure 3: Variation of tensile strength with helical angle for various (n, m) zigzag SWCNTs and (n, n) armchair SWCNTs.

3.3 Effect of vacancy defects on mechanical properties of SWCNTs

This section considers the effect of vacancy defects on the tensile strength of two typical SWCNTs. In performing the MS simulations, the vacancies were randomly distributed within the two nanotubes using the following procedure: (i) a vacancy percentage was specified in the range 3∼24%, (ii) the vacancy percentage was applied to the total number of atoms within the simulation system in order to calculate the total number of vacancies, (iii) the vacancies were numbered sequentially, (iv) the positions of the vacancies were derived by random distributions, and (v) the atoms and the vacancies were converted to their actual positions in a relaxation process. Figure 4 presents the MS simulation results for the variation of the tensile strength of the (6,6) armchair and (10,0) zigzag SWCNTs as a function of the vacancy percentage. The results show that for both nanotubes, the tensile strength reduces with an increasing vacancy percentage. The results are in a good agreement with the finding of Chen *et al.* [Chen *et al.* (2007)] using molecular mechanics calculations. Moreover, of the two nanotubes, it is apparent that the tensile strength of the (10,0) zigzag SWCNT is particularly sensitive to the presence of vacancy defects.

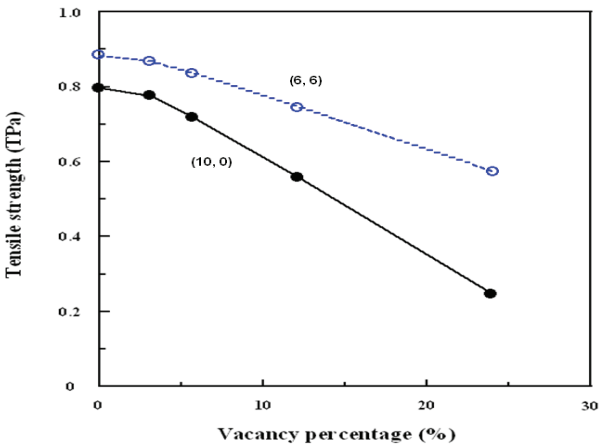

Figure 4: Variation of tensile strength with vacancy percentage in (6,6) armchair SWCNT and (10, 0) zigzag SWCNT.

4 Citations

This study has utilized Molecular Statics (MS) and Molecular Dynamics (MDs) simulations to investigate the basic mechanical properties of typical zigzag and

armchair SWCNTs under uniaxial tensile loading. The simulations have focused specifically on the effects of the wrapping angle, the tube radius and the vacancy percentage on the tensile strength, bond length and bond angle of the SWCNTs. The numerical results support the following conclusions:

At low temperatures (i.e. T = 0 K), the stress-strain predictions of the MS model are in good agreement with those of the MD model in both the elastic and the plastic deformation regimes. Moreover, the exclusion of thermal effects by the MD model when computing the relaxed atomic configuration provides a realistic interpretation of the physical mechanisms at work in practical low-temperature stress-strain tests, in which no more than a minor temperature rise is induced during the deformation process. Overall, the present results show that the MS simulation approach provides an accurate, low-cost alterative to conventional MD simulations for analyzing the mechanical properties of SWCNTs and similar micro- and nanoscale structures.

The structural deformation of SWCNTs at strains beyond the elastic limit is significantly dependent upon the helicity of the tube. Moreover, the tensile strength of SWCNTs is relatively insensitive to size effects at low values of the tube radius, but increases significantly as the diameter of the tube is increased beyond a value of approximately 6.7 nm.

The tensile strength of armchair and zigzag SWCNTs reduces as the percentage of vacancy defects increases. Of the two SWCNTs, it is apparent that the tensile strength of the (10,0) zigzag SWCNT is particularly sensitive to the presence of vacancy defects.

Acknowledgement: The authors gratefully acknowledge the support of the National Science Council of Taiwan No. NSC 95-2120-M- 194-001 and NSC 95-2120-M-194-004. The support of AFOSR under Contract No. FA4869-06-1-0056 AOARD 064053 is also acknowledged.

References

Bethune, D. S.; Klang, C. H.; Devries, M. S.; Gorman, G.; Savoy, R. ;Vazquez, J. (1993): Cobalt-catalysed growth of carbon nanotubes with single-atomic-layer walls, *Nature*, Vol. 363, pp. 605-607.

Brenner, D. W. (1990): Empirical potential for hydrocarbons for use in simulating the chemical vapor deposition of diamond films, *Physical Review B*, vol. 42, pp. 9458-9471.

Chakrabarty, A.; Cagin, T. (2008): Computational studies on mechanical and thermal properties of carbon nanotube based nanostructures, *CMC: Computers, Materials & Continua*, vol. 7, No. 3, pp. 167-190.

Chang, L.; Chen, Y. C. (2007): Is the molecular statics method suitable for the study of nanomaterials? A study case of nanowires, *Nanotechnology*, vol. 18, pp. 315701.

Chen, W. H.; Cheng, H. C.; Hsu, Y. C. (2007): Mechanical properties of carbon nanotubes using molecular dynamics simulations with the inlayer van der Waals interactions, *CMES: Computer Modeling in Engineering and Sciences*, vol. 20, pp. 123-145.

Cheng, H. M.; Li, F.; Su, G.; Pan, H. Y.; He, L. L.; Sun, X. (1998): Large-scale and low-cost synthesis of single-walled carbon nanotubes by the catalytic pyrolysis of hydrocarbons, *Applied Physics Letters*, vol. 72, pp. 3282-3284.

Cheng, H. M.; Li, F.; Sun, X.; Brown, S. D. M.; Pimenta, M. A.; Marucci, A. (1998): Bulk morphology and diameter distribution of single-walled carbon nanotubes synthesized by catalytic decomposition of hydrocarbons, *Chemical Physics Letters*, Vol. 289, pp. 602-610.

Cheong, W. C. D.; Zhang, L. C.; Tanaka, H. (2001): Some essentials of simulation nano-surfacing processes using the molecular dynamics method, *Key Engineering Materials*, vol. 196, pp. 31-42.

Ebbesen, T. W.; Ajayan, P. M. (1992): Large-scale synthesis of carbon nanotubes, *Nature*, vol. 358, pp. 220-222.

Grimm, D.; Venezuela, P.; Latgé, A. (2005): Thermal and mechanical stability of Y-shaped carbon nanotubes, *Physical Review B*, vol. 71, pp. 155425.

Iijima, S. (1991): Helical microtubules of graphitic carbon, *Nature*, vol. 21, pp. 56-58.

Iijima, S; Ichlhashi, T. (1993): Single-shell carbon nanotubes of 1-nm diameter, *Nature*, vol. 363, pp. 603-605.

Jang, I.; Sinnott, S. B.; Danailov, D.; Keblinski, P. (2004): Molecular dynamics simulation study of carbon nanotube welding under electron beam irradiation, *Nano Letters*, vol. 4, pp. 109-114

Jeng, Y. R.; Tsai, P. C.; Fang, T. H. (2007): Experimental and numerical investigation into buckling instability of carbon nanotube probes under nanoindentation, *Applied Physics Letters*, vol. 90, pp. 161913.

Jeng, Y. R.; Tsai, P. C.; Fang, T. H. (2004): Molecular dynamics investigation of the mechanical properties of gallium nitride nanotubes under tension and fatigue, *Nanotechnology*, vol. 15, pp. 1737-1744.

Jeng, Y. R.; Tsai, P. C.; Fang, T. H. (2004): Effects of temperature and vacancy defects on tensile deformation of single-walled carbon nanotubes, *Journal of Physics and Chemistry of Solids*, vol. 65, pp. 1849-1856.

Jeng, Y. R.; Kao, W. C.; Tsai, P. C. (2007): Investigation into the mechanical contact behavior of single asperities using static atomistic simulations, *Applied Physics Letters*, vol. 91, pp. 91904.

Jeng, Y. R.; Su, C. C.; Tan, C. M. (2006): An investigation of nanoscale tribological characteristics for different geometrical sliding systems, *Materials Science Forum*, vol. 507, pp. 1045-1050.

Jeng, Y.R.; Tsai, P. C. (2007): Experimental and numerical investigation into buckling instability of carbon nanotube probes under nanoindentation, *Applied Physics Letters*, vol. 90, pp. 161913.

Jeng, Y. R.; Tsai, P. C.; Fang T. H. (2004): Molecular-dynamics studies of bending mechanical properties of empty and C_{60}-filled carbon nanotubes under nanoindentation, *Journal of Chemical Physics*, vol. 122, pp. 224713.

Jeng, Y. R.; Tan, C. M. (2002): Computer simulation of tension experiments of a thin film using an atomic model, *Physical Review B*, vol. 65, pp. 174107.

Jeng, Y. R.; Tan, C. M. (2004a): Theoretical study of dislocation emission around a nanoindentation using a static atomistic model, *Physical Review B*, vol. 69, pp. 104109.

Jeng, Y. R.; Tan, C. M. (2004b): Study of nanoindentation using FEM atomic model, *ASME Journal of Tribology*, vol.126, pp. 767-774.

Jeng, Y. R.; Tan, C. M. (2005): Static atomistic simulations of nanoindentation and determination of nanohardness, *ASME Journal of Applied Mechanics*, vol. 72, pp. 738-743.

Jeng, Y. R.; Tan, C. M. (2006): Investigation into the nanoindentation size effect using static atomistic simulations, *Applied Physics Letters*, vol. 89, pp. 251901.

Journet, C.; Bernier, P. (1998): Production of carbon nanotubes, *Applied Physics A*, vol. 67, pp.1-9.

Lau, K. T.; Chong, G.; Gao, G. H. (2004): Novel in situ synthesis of MWNTs-hydroxyapatite composites, *Carbon*, vol. 42, pp. 423-426.

Liu, C. L.; Plimpton, S. J. (1995): Molecular-statics and molecular-dynamics study of diffusion along [001] tilt grain boundaries in Ag, *Physical Review B*, vol. 51, pp. 4523-4529.

Lu, J. P. (1997): Elastic properties of carbon nanotubes and nanoropes. *Physical Review Letters*, vol. 79, pp. 1297-1300.

Nardelli, M. B.; Yakobson, B. I.; Bernholc, J. (1998): Brittle and ductile behavior in carbon nanotubes, *Physical Review Letters*, vol. 81, pp. 4656-4659.

Ogata, S.; Shibutani, Y. (2003): Ideal tensile strength and band gap of single-

walled carbon nanotubes, *Physical Review B*, vol. 68, pp.165409.

Orlikowski, D.; Nardelli, M. B.; Bernholc, J.; Roland, C. (1999): Ad-dimers on strained carbon nanotubes: A new Route for quantum dot formation? *Physical Review Letters*, vol. 83, pp. 4132-4135.

Ozaki, T.; Iwasa, Y.; Mitani, T. (2000): Stiffness of single-walled carbon nanotubes under large strain, *Physical Review Letters*, vol. 84, pp. 1712-1715.

Qiu, J.; Li, Y.; Wang, Y.; Wang, T.; Zhao, Z.; Zhou, Y. (2003): High-purity single-wall carbon nanotubes synthesized from coal by arc discharge, *Carbon*, vol. 41, pp. 2170-2173.

Robertson, D. H,; Brenner, D. W.; Mintmire, J. W. (1992): Energetics of nanoscale graphitic tubules, *Physical Review B*, vol. 45, pp. 12592-12595.

Shen, S.; Atluri, S. N. (2004a): Computational nano-mechanics and multi-scale simulation, *CMC: Computers, Materials & Continua*, vol. 1, No. 1, pp. 59-90.

Shen, S.; Atluri, S. N. (2004b): Atomic-level stress calculation and continuum-molecular system equivalence, *CMES: Computer Modeling in Engineering and Sciences*, vol. 6, pp. 91-104.

Tersoff, J. (1986): New empirical model for the structural properties of silicon, *Physical Review Letters*, vol. 56, pp. 632-635.

Tersoff, J. (1988): Empirical interatomic potential for carbon, with applications to amorphous carbon, *Physical Review Letters*, vol. 61, pp. 2879-2882.

Tersoff, J.; Ruoff, R. S. (1994): Structural properties of a carbon-nanotube crystal, *Physical Review Letters*, vol. 73, pp. 676-679.

Thess, A.; Lee, R.; Nikalaev, P.; Dai, H.; Petit, P.; Robert, J. (1996): Crystalline ropes of metallic carbon nanotubes, *Science*, vol. 273, pp. 483-487.

Xie, G. Q.; Long, S. Y. (2006): Elastic vibration behaviors of carbon nanotubes based on micropolar mechanics, *CMC: Computers, Materials & Continua*, vol. 4, No. 1, pp. 11-20.

Xie, G. Q.; Han, X.; Long, S. Y. (2007): Characteristic of waves in a multi-walled carbon nanotube, *CMC: Computers, Materials & Continua*, vol. 6, No. 1, pp. 1-12.

Yakobson, B. I.; Brabec, C. J.; Bernholc, J. (1997): High strain rate fracture and C-chain unraveling in carbon nanotubes, *Computational Materials Science*, vol. 8, pp. 341-348.

Yakobson, B. I.; Brabec C. J.; Bernholc, J. (1996): Nanomechanics of carbon tubes: instabilities beyond linear response, *Physical Review Letters*, vol. 76, pp. 2511-2514.

Yu, M.F.; Files B. S.; Arepalli, S.; Ruoff, R. S. (2000a): Tensile loading of ropes

of single wall carbon nanotubes and their mechanical properties, *Physical Review Letters*, vol. 84, pp. 5552-5555.

Yu, M. F.; Lourie, O.; Dyer, M. J.; Moloni, K.; Kelly, T. F.; Ruoff, R. S. (2000b): Strength and breaking mechanism of multi-walled carbon nanotubes under tensile load, *Science*, vol. 287, pp. 637-640.

Zhang, L. C.; Tanaka, H. (1999): On the mechanics and physics in the nano-indentation of silicon mono- crystals,*JSME International Journal*, *Series A*, vol. 42, pp. 546-559.

Zhang, P.; Lammert, P. E.; Crespi, V. H. (1998): Plastic deformations of carbon nanotubes, *Physical Review Letters*, vol. 81, pp. 5346-5349.

Zhao, X.; Ohkohchi, M; Wang, M.; Iijima, S.; Ichihashi, T.; Ando, Y. (1997): Preparation of high-grade carbon nanotubes by hydrogen arc discharge, *Carbon*, vol. 35, pp. 775-781.

Zhao, Y.; Smalley, R. E.; Yakobson, B. I. (2002): Topology, energetics, and molecular dynamics?coalescence of fullerene cages: simulation, *Physical Review B*, vol. 66, pp. 195409.

Zhou, L. G.; Shi, S. Q. (2002): Molecular dynamic simulations on tensile mechanical properties of single-walled carbon nanotubes with and without hydrogen storage, *Computational Materials Science*, vol. 23, pp. 166-174.